Phase-insensitive storage of coherences by reversible mapping onto long-lived populations

Simon Mieth,[1] Genko T. Genov,[1] Leonid P. Yatsenko,[2] Nikolay V. Vitanov,[3] and Thomas Halfmann[1]

[1]*Institut für Angewandte Physik, Technische Universität Darmstadt, Hochschulstrasse 6, 64289 Darmstadt, Germany*

[2]*Institute of Physics, National Academy of Sciences of Ukraine, Prospect Nauki 46, Kiev-39, 03650, Ukraine*

[3]*Department of Physics, St. Kliment Ohridski University of Sofia, 5 James Bourchier Boulevard, 1164 Sofia, Bulgaria*

We theoretically develop and experimentally demonstrate a coherence population mapping (CPM) protocol to store atomic coherences in long-lived populations, enabling storage times far beyond the typically very short decoherence times of quantum systems. The amplitude and phase of an atomic coherence is written onto the populations of a three-state system by specifically designed sequences of radiation pulses from two coupling fields. As an important feature, the CPM sequences enable a retrieval efficiency, which is insensitive to the phase of the initial coherence. The information is preserved in every individual atom of the medium, enabling applications in purely homogeneously or inhomogeneously broadened ensembles even when stochastic phase jumps are the main source of decoherence. We experimentally confirm the theoretical predictions by applying CPM for storage of atomic coherences in a doped solid, reaching storage times in the regime of 1 min.

I. INTRODUCTION

Storage of information in quantum systems typically relies on atomic coherences, i.e., coherent superpositions of quantum states. During the storage time, atomic coherences suffer from decoherence, i.e., stochastic and irreversible variation of their phase. This destroys the encoded information. There are some general approaches available to deal with decoherence, e.g., dynamical decoupling [1–4]. However, these protocols are rather complicated, often difficult to implement, and very sensitive to fluctuations in the experimental parameters. Another drawback of protocols that store coherence information in populations and rely on collective emission, e.g., stimulated photon echo [5,6], is that they do not preserve the information equally well in each individual atom. In addition, all these protocols either fail or cannot perform phase-insensitive storage when stochastic phase jumps are the main source of decoherence.

In this work we theoretically develop and experimentally implement a coherence storage protocol, which maps (writes) a qubit coherence onto three long-lived populations by a short sequence of coherent radiation pulses. After some storage time, we map (read) the populations back onto the qubit coherence by another short pulse sequence. The possible storage time is limited only by the population lifetime of the system, which typically exceeds the decoherence time by far. As a prominent feature of our coherence population mapping (CPM) protocol, each single atom in the medium carries and maintains the full information about the initial coherence, unlike other protocols, e.g., the well-established stimulated photon echo (SPE) [5,6]. As a result, the storage efficiency of CPM does not depend upon the phase of the stored coherence. Unlike other protocols with reduced sensitivity to the phase of the coherence, e.g., Knill dynamical decoupling [4], CPM does not require complicated and error-sensitive additional fields during storage, which typically also lead to reduced efficiency.

Beyond the theoretical proposal, we also present a convincing experimental demonstration of CPM in a rare-earth-ion doped crystal. However, our approach is not limited to this specific medium. CPM enables applications in any ensemble of inhomogeneously or purely homogeneously broadened three-state systems, e.g., atomic vapors, NMR spin systems, doped solids, or quantum dots. The ability to store the full information in each system also enables partial readout of specific frequency components stored in inhomogeneously broadened media, e.g., for (radio) frequency analysis. CPM thus allows a broad spectrum of applications in various systems.

II. THEORY OF CPM

We consider a three-state system driven coherently by two radiation fields. Any type of three-level scheme with two allowed transitions is applicable for CPM (see Fig. 1). Without loss of generality, the following analysis focuses on the ladder system (Fig. 1, center), corresponding to our specific experiment. Initially, the system is prepared in an arbitrary coherent superposition of states $|1\rangle$ and $|2\rangle$, i.e., it serves as a memory for information encoded in this coherence. We also allow for the general case that some incoherent population may remain in state $|3\rangle$, but the coherences $\rho_{13} = \rho_{23} = 0$ are completely dephased. The aim of CPM is to transfer the information stored in the coherence ρ_{12} (amplitude and phase) to the long-lived populations in states $|1\rangle$, $|2\rangle$, and $|3\rangle$, and back again. This enables storage of the fragile coherences in robust, long-lived populations. Next, we derive simple pulse sequences which perform this task. The pulse areas and relative phases serve as control parameters. The dynamics are described by the Liouville equation $i\hbar\partial_t\rho(t) = [\mathbf{H}(t),\rho(t)]$,
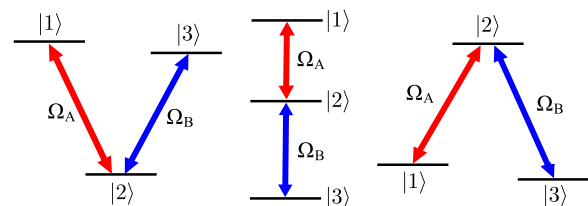
FIG. 1. Different types of three-level schemes to implement CPM. The initial coherence is on transition A.

TABLE I. CPM "write" and "read" sequences. Each single pulse A, B is defined by its pulse area Θ and phase ϕ. The values $\phi_{\rm w}$ and $\phi_{\rm r}$ are arbitrary phases of the "write" and "read" pulse B (or A), and ϕ is an arbitrary overall phase shift of the whole reading sequence. Another parameter is the specific pulse area $\theta = \arccos{(-1/3)} \approx 0.608\pi$.

Write sequences	Read sequences
$A_0(\pi/2)B_{\phi_{\rm w}}(\theta)A_{\pm\pi/2}(\pi/2)$	$[A_{\pm\pi/2}(\pi/2)B_{\phi_{\rm r}}(\theta)A_0(\pi/2)]_\phi$
$B_0(\pi/2)A_{\phi_{\rm w}}(\theta)B_{\pm\pi/2}(\pi/2)$	$[B_{\pm\pi/2}(\pi/2)A_{\phi_{\rm r}}(\theta)B_0(\pi/2)]_\phi$

where $\rho(t)$ is the density matrix. We assume sufficiently short resonant radiation pulses, so we can neglect decoherence and population decay. The Hamiltonian in rotating-wave approximation (RWA) reads

$$\mathbf{H}(t) = \frac{\hbar}{2}\big[\Omega_{\rm A}(t)e^{i\phi_{\rm A}}\Pi_{12} + \Omega_{\rm B}(t)e^{i\phi_{\rm B}}\Pi_{23} + {\rm H.c.}\big], \quad (1)$$

where $\Pi_{jk} = |j\rangle\langle k|$ is a projection operator; Ω are Rabi frequencies at the transition $|1\rangle \leftrightarrow |2\rangle$ (which we term "A") and the transition $|2\rangle \leftrightarrow |3\rangle$ (which we term "B"); and ϕ are the phases of the Rabi frequencies. Field A is at the transition with the initial coherence $\rho_{12}^{\rm in}$.

The temporal evolution is described by the propagator $\mathbf{U}^{\rm P}$, connecting the density matrices at the initial and final times of the interaction by $\rho^{\rm fin} = \mathbf{U}^{\rm P}\rho^{\rm in}(\mathbf{U}^{\rm P})^\dagger$, i.e.,

$$\mathbf{U}_{\phi_{\rm P}}^{\rm P}(\Theta_{\rm P}) = \cos{(\Theta_{\rm P}/2)}(\Pi_{jj} + \Pi_{kk}) + \Pi_{ll}$$
$$+ [ie^{i\phi_{\rm P}}\sin{(\Theta_{\rm P}/2)}\Pi_{jk} + {\rm H.c.}], \ l \neq j,k. \quad (2)$$

$\mathbf{U}^{\rm P}$ with $P = A, B$ is the propagator of a single pulse A or B, and $\Theta \equiv \int_{t_i}^{t_f} \Omega(t)dt$ is the respective pulse area. The propagator of a sequence of pulses, e.g., an ABA sequence, denoted $A_{\phi_1}(\Theta_1)B_{\phi_2}(\Theta_2)A_{\phi_3}(\Theta_3)$, is

$$\mathbf{U}^{\rm ABA} = \mathbf{U}_{\phi_3}^A(\Theta_3) \cdot \mathbf{U}_{\phi_2}^B(\Theta_2) \cdot \mathbf{U}_{\phi_1}^A(\Theta_1), \quad (3)$$

where values in brackets give the pulse areas, and subscripts give the phases. The propagator of a BAB sequence is obtained similarly. We use the exact analytic solutions for the propagators to find the appropriate pulse areas and phases which allow phase-insensitive storage and retrieval of $\rho_{12}^{\rm in}$ for every atom.

In the CPM "write" process, we apply an ABA sequence (or alternatively, a BAB sequence) of resonant pulses, with parameters given in Table I. The "write" process produces a unitary transformation where the matrix elements of $\rho^{\rm in}$ are mixed up in all elements of the density matrix after the writing, i.e., $\rho^{\rm w} = \mathbf{U}^{\rm w}\rho^{\rm in}(\mathbf{U}^{\rm w})^\dagger$, where $\mathbf{U}^{\rm w}$ is determined by Table I and Eq. (3). Hence, we map the atomic coherence onto an incoherent distribution of populations—which nevertheless contains all information of the initial coherence.

The system evolves freely now and dephases completely during the storage time $\Delta\tau$, which shall be much longer than the decoherence time. We are then left with a completely incoherent superposition of the three storage states. We label the density matrix before the CPM "read" process and at the end of the storage time $\rho^{\rm s}$ and its elements become $\rho_{jk}^{\rm s} = 0 \ (j \neq k), \rho_{jj}^{\rm s} = \rho_{jj}^{\rm w}$, i.e., only the diagonal elements
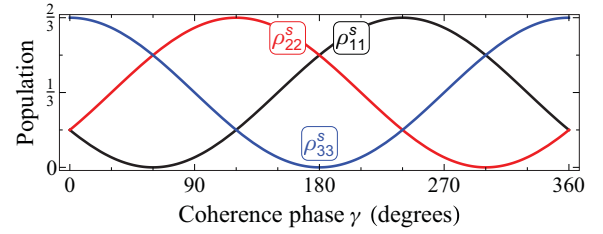
FIG. 2. Simulation of populations during storage for CPM (ABA) for different coherence phases γ. We assume for simplicity that $\rho_{11}^{\rm in} = \rho_{22}^{\rm in} = 1/2$, $\rho_{12}^{\rm in} = ie^{i\gamma}/2$.

of $\rho^{\rm w}$ are preserved. Figure 2 shows a characteristic example population distribution during storage for different phases of the coherence $\rho_{12}^{\rm in}$.

During the "read" process we apply an ABA (or a BAB) reading sequence, corresponding to the respective "write" process. The retrieved density matrix is $\rho^{\rm out} = \mathbf{U}^{\rm r}\rho^{\rm s}(\mathbf{U}^{\rm r})^\dagger$, where $\mathbf{U}^{\rm r}$ is determined by Table I and Eq. (3). The relevant density matrix elements are

$$\rho_{jj}^{\rm out} = (1/3)\big(\rho_{11}^{\rm in} + \rho_{22}^{\rm in} + \rho_{33}^{\rm in}\big), j = 1,2,3, \quad (4a)$$

$${\rm ABA:}\rho_{12}^{\rm out} = -(1/3)e^{i\phi}\rho_{12}^{\rm in}, \quad (4b)$$

$${\rm BAB:}\rho_{12}^{\rm out} = -(1/3)e^{i(\phi+\phi_{\rm r}-\phi_{\rm w})}\rho_{12}^{\rm in}, \quad (4c)$$

where the phase ϕ denotes an arbitrary, overall phase shift. The phases $\phi_{\rm w}, \phi_{\rm r}$ can be random in the ABA sequences and do not affect $\rho_{12}^{\rm out}$. They add a phase shift of $\phi_{\rm r} - \phi_{\rm w}$ to $\rho_{12}^{\rm out}$ for the BAB case. All phases can be shifted simultaneously without affecting $\rho_{12}^{\rm out}$. We note that the off-diagonal elements of the retrieved density matrix are $|\rho_{jk}^{\rm out}| = 1/3|\rho_{12}^{\rm in}|, j \neq k$. Thus, after CPM the full information about the initial coherence is distributed equally among all three coherences of the system, i.e., we can find information about the initial coherence also in the other two coherences. As an important consequence, it is possible to retrieve the initial coherence information from any of the three final coherences or to transfer the information from the initial coherence to any other transition.

We note that CPM is fundamentally different from the well-known SPE protocol for data storage in inhomogeneously broadened media [5–7]. For SPE we apply a "data" pulse, e.g., $\pi/2$, to prepare a coherence $\rho_{12}^{\rm in}$. We wait for some time T, with $T \gg 1/\Gamma_{\rm inh}$, where $\Gamma_{\rm inh}$ is the inhomogeneous linewidth of the medium, and apply a "write" process with a $A_0(\pi/2)$ pulse. After a storage time of $\Delta\tau$, we drive a "read" process with a second $A_0(\pi/2)$ pulse. A time-reversed echo of the initial preparation pulse is produced after a delay T. As a serious limitation of SPE, it does not store the full information from the initial coherence. For example, if $T = 0$ the retrieved coherence in SPE is $\rho_{12}^{\rm out} = -i{\rm Im}(\rho_{12}^{\rm in})$, i.e., only the imaginary part of $\rho_{12}^{\rm in}$ is preserved, and its full magnitude can be retrieved only when it has a specific phase. In the case $T \gg 1/\Gamma_{\rm inh}$, the SPE retrieval efficiency varies for the different atoms. CPM does not suffer from such problems. CPM is phase insensitive and preserves equally well the coherence of each single atom, even when $T = 0$. In the following we experimentally demonstrate these important advantages of CPM.
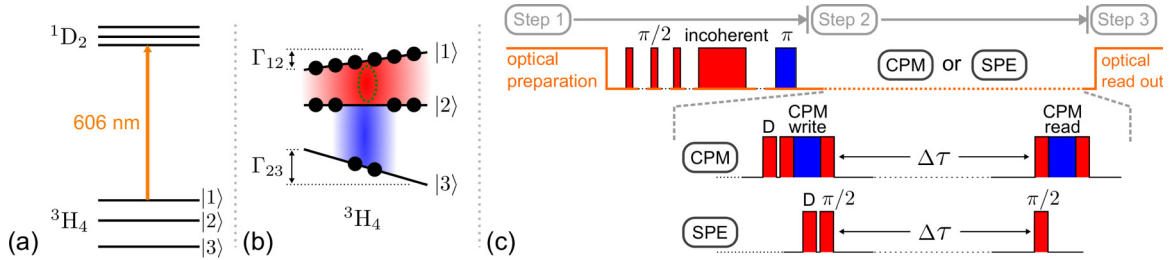
FIG. 3. (a, b) Optical and rf excitation scheme in PrYSO. Black circles indicate the population distribution after preparation. (c) Upper row: Sequences of optical and rf pulses, applied for optical preparation, generation of an rf pit, and optical readout. Lower rows: rf sequences for CPM or SPE. Red (blue) color depicts pulses A (B). D is the data pulse.

III. EXPERIMENT

The experiment is implemented in praseodymium ions doped into a yttrium orthosilicate crystal (termed PrYSO). PrYSO exhibits long-lived hyperfine ground states in the $^3H_4$ manifold and an optically excited state $^1D_2$ [see Fig. 3(a)]. The optical transition is inhomogeneously broadened to $\Gamma_{\mathrm{opt}} \approx 7\,\mathrm{GHz}$. We use a solid-state laser system [8] to prepare the medium and read out the restored coherence. The hyperfine states $|1\rangle$, $|2\rangle$, and $|3\rangle$ in the $^3H_4$ manifold have transition frequencies in the rf range, decoherence time $T_2 = 500\,\mu\mathrm{s}$, and population relaxation times of $T_1 = 8.7\,\mathrm{s}$ at transition A ($|1\rangle \leftrightarrow |2\rangle$) and $T_1 = 109\,\mathrm{s}$ at transition B ($|2\rangle \leftrightarrow |3\rangle$). Population relaxation is mainly caused by phonons. The variation in relaxation times is due to the different transition moments between the three levels involved. This is a well-known issue for rare-earth doped solids (see, e.g., [9] and references therein).

We operate at cryogenic temperatures around 4 K. The rf transition frequencies are $\omega_{12} \equiv \omega_A = 2\pi \times 10.19\,\mathrm{MHz}$ and $\omega_{23} \equiv \omega_B = 2\pi \times 17.31\,\mathrm{MHz}$, both inhomogeneously broadened to $\Gamma_{12} \approx 2\pi \times 40\,\mathrm{kHz}$ and $\Gamma_{23} \approx 2\pi \times 80\,\mathrm{kHz}$ (FWHM) [see Fig. 3(b)]. An arbitrary wave-form generator (Tektronix AWG5014) and an amplifier (Mini-Circuits LZY-22+) provide rf pulses with Rabi frequencies up to $\Omega_A = 2\pi \times 145\,\mathrm{kHz}$ and $\Omega_B = 2\pi \times 50\,\mathrm{kHz}$. All pulses have rectangular temporal intensity profiles with durations of $1.7\,\mu\mathrm{s}$ for pulses $A(\pi/2)$ and $6\,\mu\mathrm{s}$ for $B(\theta)$.

The experiment consists of three steps [see Fig. 3(c)]: (1) We prepare the system by optical pumping in order to empty state $|3\rangle$ (see also [10,11]), as well as by applying a sequence of $A(\pi/2)$ and incoherent rf pulses to provide equal populations in states $|1\rangle$ and $|2\rangle$, and a pulse $B(\pi)$ to transfer population to state $|3\rangle$ [see Fig. 3(b)]. Pulse B has a spectral width smaller than Γ_{23}, thus creating a selective population difference in a small spectral region of the inhomogeneous manifold. We call this an rf spectral pit, with a spectral width determined by pulse B. Thus, the pit is spectrally matched to all further pulses B. An initial "data" pulse A will then generate coherences exclusively in ensembles, prepared by the pulse $B(\pi)$ before. This is important to reduce possible noise induced from ensembles outside the bandwidth of pulse B. We have developed the rf spectral pit technique for this specific experiment in doped solids, but it will be of relevance also to other experiments. We note that in general CPM does not affect the multiplexing capacities of the medium. Nevertheless, the mapping (optical or rf) pulses have to cover the bandwidth of the stored coherences to implement time or frequency multiplexing. In our specific experiment, only a technical limitation of rf power for pulses B reduces the frequency multiplexing capacity in the rf regime. (2) In the second step, we initiate the atomic coherence $\rho_{12}^{\mathrm{in}} = i|\rho_{12}^{\mathrm{in}}|\exp(i\gamma)$ by a first "data" pulse $A_\gamma(\pi/2)$. The phase of the coherence is determined by the phase of the data pulse. Afterwards we apply CPM sequences to map the coherence ρ_{12}^{in} onto populations and back again. Specifically, we use the ABA ($\phi = 0$) sequences from Table I. For comparison, we apply SPE ($T = 0$) sequences [Fig. 3(c)]. The time delay between "write" and "read" sequences defines the storage time $\Delta\tau$, desired to be as long as possible. (3) In a third step, we detect restored coherences by Raman heterodyne detection [12], driven by the same laser as applied for optical preparation.

We perform two experiments to show the key features of CPM. First, we vary the phase γ of the initial coherence from $\gamma = 0°$ to $\gamma = 360°$ to prove phase-insensitive storage by CPM. Figure 4 shows the retrieved signal after a storage time $\Delta\tau = 4\,\mathrm{ms}$ for CPM, and SPE for comparison. As the data clearly indicate, CPM yields constant retrieval efficiency, i.e., independent of the initial coherence phase. On the other hand, SPE suffers from strong oscillations of the retrieval efficiency vs the phase of the initial coherence. For specific phases ($\gamma = 160°$ and $\gamma = 340°$) the retrieved signal is strong. However, for phases $\gamma = 70°$ and $\gamma = 250°$, the retrieved signal with SPE vanishes entirely. This strong phase dependence of the retrieval efficiency is a well-known disadvantage of SPE, as well as of many rephasing protocols. It is an obstacle to information processing in any medium which requires efficient restoration of an initial coherence with an arbitrary phase. CPM offers a solution here.
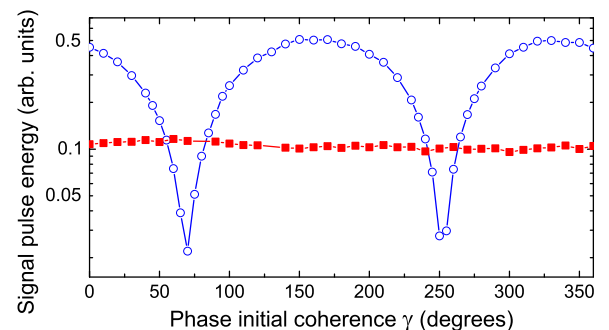
FIG. 4. Retrieved signal vs initial coherence phase after CPM (red, solid squares) or SPE (blue, hollow circles).
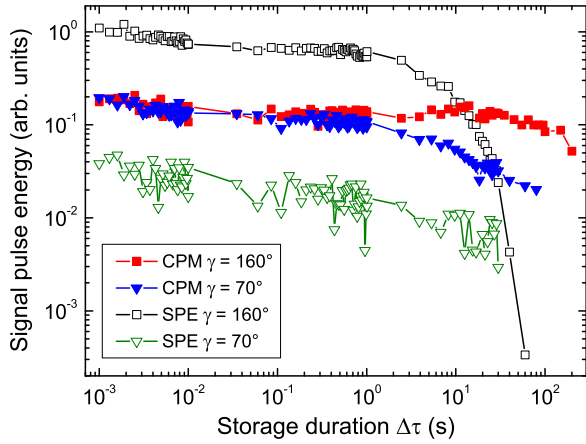
FIG. 5. Retrieved signal vs storage duration for CPM, with an initial coherence phase of 160° (red, solid squares) or 70° (blue, solid triangles), and for SPE, with an initial coherence phase of 160° (black, hollow squares) or 70° (green, hollow triangles). Note the logarithmic scales.

In a second measurement we confirm the capability of CPM to maintain a signal for very long storage times, limited only by population relaxation. Figure 5 shows retrieved signals after CPM and SPE vs the storage duration $\Delta\tau$. We perform the measurement for two phases of the initial coherence, $\gamma = 70°$ and $\gamma = 160°$, which show the highest difference in retrieval efficiency for SPE. CPM reaches long storage times of as many as 10 s for any arbitrary phase of the initial coherence. This clearly outperforms SPE, i.e., we retrieve only a very small SPE signal for an initial coherence with a phase $\gamma = 70°$, and a high signal at $\gamma = 160°$ only for shorter storage times. The SPE signals decay with a characteristic $1/e$ time of $\tau_{\mathrm{SPE}} \approx 3.2$ s. Even at the optimal phase of $\gamma = 160°$, the SPE signal vanishes completely after $\Delta\tau \approx 30$ s, whereas CPM still yields detectable signals for both phases at very long storage times. The CPM signal for the coherence phase of $\gamma = 70°$ decays with a $1/e$ time $\tau_{\mathrm{CPM}}^{70} \approx 5.4$ s and the CPM signal at a phase of $\gamma = 160°$ with $\tau_{\mathrm{CPM}}^{160} \approx 175$ s. We note that the decay of the CPM signals is no single exponential, because the protocol involves not one, but two transitions with different population relaxation times. The different decay times for

the CPM signals at the two phases are due to the different population relaxation times between the three hyperfine states of PrYSO. As the population distributions after the CPM "write" process vary with the initial coherence phase (see Fig. 2), the decay rates of the CPM signals also vary with the initial phase due to the different relaxation rates of the two transitions. Without population relaxation, CPM would yield uniform retrieval efficiency [see Eqs. (4)]. This is not valid in the case of population relaxation. The population difference on transition A is very small for a phase of $\gamma = 160°$ compared to $\gamma = 70°$, and vice versa for transition B. Consequently, CPM for $\gamma = 160°$ benefits from slow relaxation of transition B, resulting in a longer storage time.

IV. CONCLUSION

We theoretically developed and experimentally demonstrated a coherence population mapping (CPM) protocol for storage of coherences in long-lived populations, permitting storage durations well beyond the decoherence time of a system. The technique does not require complex setups beyond radiation sources to coherently drive the relevant transitions and is applicable to any three-state medium. This makes CPM a quite general and experimentally feasible concept for coherence storage. As important advantages, CPM preserves equally well the coherence of every individual atom (i.e., the full information is equally stored in each single atom), and the efficiency of the protocol does not depend upon the initial coherence phase. We experimentally confirmed the theoretical predictions by applying CPM to store atomic coherences in a PrYSO crystal. The experiment demonstrates the superior performance of CPM, i.e., equal storage efficiency for any arbitrary phase of the initial coherence, and storage times far beyond the decoherence time of the system, reaching the minute regime.

[1] G. Heinze, C. Hubrich, and T. Halfmann, Phys. Rev. Lett. **111**, 033601 (2013).

[2] M. Zhong, M. P. Hedges, R. L. Ahlefeldt, J. G. Bartholomew, S. E. Beavan, S. M. Wittig, J. J. Longdell, and M. J. Sellars, Nature (London) **517**, 177 (2015).

[3] L. Viola and S. Lloyd, Phys. Rev. A **58**, 2733 (1998).

[4] A. M. Souza, G. A. Álvarez, and D. Suter, Phys. Rev. Lett. **106**, 240501 (2011); M. Lovrić, D. Suter, A. Ferrier, and P. Goldner, *ibid.* **111**, 020503 (2013).

[5] T. W. Mossberg, R. Kachru, S. R. Hartmann, and A. M. Flusberg, Phys. Rev. A **20**, 1976 (1979).

[6] W. Tittel, M. Afzelius, T. Chanelière, S. Kröll, S. Moiseev, and M. Sellars, Laser Photonics Rev. **4**, 244 (2010).

[7] N. Sangouard, C. Simon, J. Minár, M. Afzelius, T. Chanelière, N. Gisin, J.-L. Le Gouët, H. de Riedmatten, and W. Tittel, Phys. Rev. A **81**, 062333 (2010).

[8] S. Mieth, A. Henderson, and T. Halfmann, Opt. Express **22**, 11182 (2014).

[9] R. M. Shelby, R. M. Macfarlane, and C. S. Yannoni, Phys. Rev. B **21**, 5004 (1980).

[10] F. Beil, J. Klein, G. Nikoghosyan, and T. Halfmann, J. Phys. B **41**, 074001 (2008).

[11] M. Nilsson, L. Rippe, S. Kröll, R. Klieber, and D. Suter, Phys. Rev. B **70**, 214116 (2004).

[12] N. C. Wong, E. S. Kintzer, J. Mlynek, R. G. DeVoe, and R. G. Brewer, Phys. Rev. B **28**, 4993 (1983).